

**Heavy sterile neutrinos in tau decays and the MiniBooNE anomaly**Claudio Dib,<sup>1</sup> Juan Carlos Helo,<sup>1</sup> Martin Hirsch,<sup>2</sup> Sergey Kovalenko,<sup>1</sup> and Ivan Schmidt<sup>1</sup><sup>1</sup>*Universidad Técnica Federico Santa María, Centro-Científico-Tecnológico de Valparaíso, Casilla 110-V, Valparaíso, Chile*<sup>2</sup>*AHEP Group, Instituto de Física Corpuscular-C.S.I.C./Universidad de Valencia Edificio de Institutos de Paterna, Apartado 22085, E-46071 Valencia, Spain*

(Received 28 October 2011; published 6 January 2012)

Current results of the MiniBooNE experiment show excess events that indicate neutrino oscillations, but only if one goes beyond the standard 3 family scenario. Recently a different explanation of the events has been given, not in terms of oscillations but by the production and decay of a massive sterile neutrino with large transition magnetic moment. We study the effect of such a sterile neutrino in the rare decays  $\tau^- \rightarrow \mu^- \mu^+ \pi^- \nu$  and  $\tau^- \rightarrow \mu^- \mu^+ e^- \nu \nu$ . We find that searches for these decays, featuring displaced vertices between the  $\mu^-$  and the other charged particles, constitute reliable tests for the existence of the sterile neutrino proposed to explain the MiniBooNE anomaly. These searches could be done with already existing experimental data.

DOI: 10.1103/PhysRevD.85.011301

PACS numbers: 14.60.St, 13.15.+g, 13.35.Dx, 13.35.Hb

In 1996, the Liquid Scintillator Neutrino Detector (LSND) experiment presented evidence of  $\bar{\nu}_\mu \rightarrow \bar{\nu}_e$  transitions, which were not consistent with the global neutrino data [1]. This experiment used  $\bar{\nu}_\mu$  produced in the beam stop of a proton accelerator. The  $\bar{\nu}_\mu$  energy distribution peaked near 55 MeV, with a mean energy near 100 MeV. The search for  $\bar{\nu}_\mu \rightarrow \bar{\nu}_e$  was based on the appearance of  $\bar{\nu}_e$  in the neutrino beam, detected through the reaction  $\bar{\nu}_e p^+ \rightarrow e^+ n$ , resulting in a relativistic  $e^+$  [1]. With the aim to confirm this anomaly, the MiniBooNE experiment was designed to search for  $\nu_\mu \rightarrow \nu_e$ , at higher energies than the LSND experiment (namely above 475 MeV, peaked near 600 MeV and average near 800 MeV), but at similar  $L/E$ ,  $L$  being the distance traveled by the neutrinos and  $E$  their energy. In this search the MiniBooNE experiment did not find positive signals [2]. However, looking at lower energies (below 475 MeV) the MiniBooNE collaboration has observed an excess of electron-like events in the energy distribution of charge-current quasielastic electron neutrino events [3]. Recently, the MiniBooNE collaboration, in searches for  $\bar{\nu}_\mu \rightarrow \bar{\nu}_e$  oscillations, has also found that the antineutrino data have an anomalous low-energy excess similar to that of the neutrino data [4].

Clarification of the MiniBooNE and LSND anomalies is a very important task, since it seems to require new physics that cannot be explained by the Standard Model. Over the last decade, many explanations have been proposed, including new oscillation physics [5] and production of photons in neutrino scattering events [6,7]. Since the MiniBooNE and LSND detectors cannot differentiate between Cerenkov rings produced by electrons (positrons) or converted photons, the excess observed could come from photons instead of electrons (positrons), as assumed in the neutrino oscillation paradigm. Consequently, one of the main problems is that we do not know whether the MiniBooNE and LSND excess events are both signals of

neutrino oscillations, or if any of them has a different origin.

The MicroBooNE experiment is being planned to start taking data next year in order to check the MiniBooNE anomaly [8]. It can confirm the MiniBooNE excess as well as discriminate between production of electrons or photons, and hence clarify the nature of the excess [8]. If the signals turn out to be from photons, they will not be due to neutrino oscillation but may come from the dominant radiative decay of a sterile neutrino  $N$  with mass  $m_N$ , mixing strength  $U_{\mu N}$ , and lifetime  $\tau_N$  in the respective ranges: [6,9]

$$\begin{aligned} 400 \text{ MeV} &\lesssim m_N \lesssim 600 \text{ MeV}, \\ 1 \times 10^{-3} &\lesssim |U_{\mu N}|^2 \lesssim 4 \times 10^{-3}, \\ \tau_N &\lesssim 1 \times 10^{-9} \text{ s}. \end{aligned} \quad (1)$$

This sterile neutrino is produced by  $Z^0$  exchange of the incoming  $\nu_\mu$  or  $\bar{\nu}_\mu$  with a nucleus in the detector [6]. In turn, the subsequent radiative decay of  $N$  requires a transition magnetic moment within the following range, in order to explain the MiniBooNE signal:

$$\mu_{tr} \simeq (1 - 6) \times 10^{-9} \mu_B, \quad (2)$$

where  $\mu_B$  is the Bohr magneton. These values imply that  $N$  decays dominantly in the mode  $N \rightarrow \nu \gamma$ , and therefore the total width  $\Gamma_N$  can be approximated by [10]

$$\Gamma_N \sim \Gamma(N \rightarrow \nu \gamma) = \frac{\alpha}{8} \left( \frac{\mu_{tr}}{\mu_B} \right)^2 \left( \frac{m_N}{m_e} \right)^2 m_N, \quad (3)$$

thus constraining the sterile neutrino lifetime shown in Eq. (1) to be in the range

$$2 \times 10^{-11} \text{ s} \lesssim \tau_N \lesssim 1 \times 10^{-9} \text{ s}. \quad (4)$$

Of course, this explanation suggests that the MiniBooNE anomaly comes from a different physics than the LSND [1]

and other neutrino anomalies [11]. Motivations along this line have been proposed in [12], where it is found that the appearance and disappearance data are marginally compatible in a  $(3 + 1)$  neutrino mixing model, if we disregard the MiniBooNE data of the low-energy anomaly. Then, according to [12], the MiniBooNE excess seems to have an explanation other than neutrino oscillations.

There have also been attempts to explain the MiniBooNE and LSND anomalies simultaneously using a similar scenario with a radiative decaying sterile neutrino  $N \rightarrow \nu\gamma$ , this time using sterile neutrino masses around 60 MeV [7] (see also [13]). However, such scenario has been recently ruled out using direct searches of radiative  $K$  meson decays at ISTRA + Setup [14].

Concerning experimental tests of a sterile neutrino in the range given by the Eqs. (1), (2), and (4), direct searches using  $D_s$  decays have already been proposed [15]. Moreover, the MicroBooNE experiment could easily probe this model if they find that the MiniBooNE anomaly is due to photons and not electrons. The main purpose of this paper is to propose searches for a heavy neutrino in  $\tau$  decays, with properties described in [6] and parameters in the range given by Eqs. (1), (2), and (4).

If a sterile neutrino  $N$  with parameters in the range (1), (2), and (4) exists, it should contribute as an on-shell intermediate particle in the following  $\tau$  decays:

$$\tau^- \rightarrow \mu^- \mu^+ \pi^- \nu \quad \text{and} \quad \tau^- \rightarrow \mu^- \mu^+ e^- \nu \nu. \quad (5)$$

This means that an intermediate sterile neutrino is produced at one vertex, propagates as a free unstable particle, and then decays at certain distance at another vertex. Examples of the corresponding diagrams are given in Fig. 1. These decays could be searched for in  $\tau$  decay events with two vertices leading to very clean signals: a primary vertex from  $\tau^- \rightarrow \mu^- \nu N$  and a secondary displaced vertex either from  $N \rightarrow \mu^+ \pi^-$  (Fig. 1(a)) or from  $N \rightarrow \mu^+ e^- \nu$  (Fig. 1(b)). In the case of  $\tau^- \rightarrow \mu^- \mu^+ \pi^- \nu$ , the experimental signature  $\mu^+ \pi^-$  coming from the displaced vertex would be two charged tracks and, since they are not accompanied with a neutrino, it could be possible to reconstruct the mass of the sterile neutrino (1). This would show as a peak in invariant mass squared of the pair in the range 0.16–0.36 GeV<sup>2</sup>, thus providing an excellent cross-check of the model. The  $\tau$  decay rates in question (see Fig. 1), dominated by an on-shell sterile neutrino  $N$  in the intermediate state, are

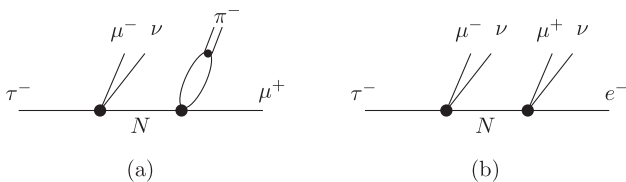


FIG. 1. Structure of the on-shell sterile neutrino  $N$  contribution to the  $\tau$  decays (5).

$$\begin{aligned} & \Gamma(\tau^- \rightarrow \{\mu^- \nu\}_1 \{\mu^+ e^- \nu\}_2) \\ & \approx \delta_N \cdot \Gamma(\tau^- \rightarrow \mu^- \bar{\nu}_\mu N) \frac{\Gamma(N \rightarrow \mu^+ e^- \bar{\nu}_e)}{\Gamma_N} \\ & + \Gamma(\tau^- \rightarrow \mu^- \nu_\tau N) \frac{\Gamma(N \rightarrow \mu^+ e^- \bar{\nu}_e)}{\Gamma_N}, \end{aligned} \quad (6)$$

$$\begin{aligned} & \Gamma(\tau^- \rightarrow \{\mu^- \nu\}_1 \{\mu^+ \pi^-\}_2) \\ & \approx \delta_N \cdot \Gamma(\tau^- \rightarrow \mu^- \bar{\nu}_\mu N) \frac{\Gamma(N \rightarrow \mu^+ \pi^-)}{\Gamma_N} \\ & + \Gamma(\tau^- \rightarrow \mu^- \nu_\tau N) \frac{\Gamma(N \rightarrow \mu^+ \pi^-)}{\Gamma_N}, \end{aligned} \quad (7)$$

where  $\delta_N = 0, 1$  for a Dirac or Majorana type of sterile neutrino  $N$ , respectively. The curly brackets  $\{\dots\}_1$  and  $\{\dots\}_2$  denote the two displaced vertices, which are distinguished experimentally. Note also that neutrinos in final states are not identifiable experimentally and could be either neutrino or antineutrino of any type. Therefore, in (6) and (7) we sum up over all possible neutrino final states. The analytical expressions for the relevant  $\tau$  and  $N$  partial decay rates are [16,17]:

$$\begin{aligned} \Gamma(\tau^- \rightarrow \mu^- \nu_\tau N) &= |U_{\mu N}|^2 \frac{G_F^2}{192\pi^3} m_\tau^5 I(z_N, z_\nu, z_\mu), \\ \Gamma(\tau^- \rightarrow l^- \bar{\nu}_l N) &= |U_{\tau N}|^2 \frac{G_F^2}{192\pi^3} m_\tau^5 I(z_N, z_\nu, z_l), \end{aligned} \quad (8)$$

$$\begin{aligned} \Gamma(N \rightarrow \mu^+ e^- \bar{\nu}_e) &= |U_{\mu N}|^2 \frac{G_F^2}{192\pi^3} m_N^5 I(y_e, y_\nu, y_\mu), \\ \Gamma(N \rightarrow \mu^+ \pi^-) &= |U_{\mu N}|^2 \frac{G_F^2}{16\pi} m_N^3 f_\pi^2 |V_{ud}|^2 F_P(y_\mu, y_\pi). \end{aligned} \quad (9)$$

Here,  $l = \mu, e$  and we have defined  $z_i = m_i/m_\tau$ ,  $y_i = m_i/m_N$ , for  $m_i = m_N, m_\nu, m_\mu, m_e, m_\pi$ ;  $f_\pi = 130$  MeV. The kinematical functions in Eqs. (8) and (9) are

$$\begin{aligned} I(x, y, z) &= 12 \int_{(x+y)^2}^{(1-z)^2} \frac{ds}{s} (s - x^2 - y^2)(1 + z^2 - s) \lambda^{1/2}(s, x^2, y^2) \\ & \times \lambda^{1/2}(1, s, z^2), \end{aligned} \quad (10)$$

$$F_P(x, y) = \lambda^{1/2}(1, x^2, y^2) [(1 + x^2)(1 + x^2 - y^2) - 4x^2]. \quad (11)$$

The  $\tau$  branching ratios in Eqs. (6) and (7) must be in the following ranges, in order to be consistent with the parameters in Eqs. (1) and (2) that explain the MiniBooNE anomaly:

$$\text{Br}(\tau^- \rightarrow \{\mu^- \nu\}_1 \{\mu^+ e^- \nu\}_2) = 2.1 \times 10^{-8} - 8.2 \times 10^{-5}, \quad (12)$$

$$\text{Br}(\tau^- \rightarrow \{\mu^- \nu\}_1 \{\mu^+ \pi^-\}_2) = 2.0 \times 10^{-9} - 1.3 \times 10^{-5}. \quad (13)$$

This is a crucial result: the branching ratios are bounded from above and also from below. Consequently, their non-observation at experimental sensitivities better than the

specified lower limits would be able to rule out the sterile neutrino hypothesis in the range (1). In these numerical evaluations we have used  $|U_{\tau N}|^2 < 10^{-2}$ , which is consistent with the best current limits in the sterile neutrino mass range (1) [16,18]. For simplicity we also set  $U_{eN} = 0$ , which is reasonable considering that  $U_{eN}$  is strongly constrained for  $m_N$  in the range of Eq. (1) [16,17].

One also should notice that these decays are identified not just by their final state, but also by their displaced vertex topology. In fact, each of these decays have another contribution from sterile neutrinos that have different vertex topology: a primary vertex  $\tau^- \rightarrow \pi^- N$ , or  $\tau^- \rightarrow e^- \nu N$  correspondingly, followed by a secondary displaced vertex  $N \rightarrow \mu^+ \mu^- \nu$ :

$$\begin{aligned} & \Gamma(\tau^- \rightarrow \{e^- \nu\}_1 \{\mu^+ \mu^- \nu\}_2) \\ & \approx \delta_N \cdot \Gamma(\tau^- \rightarrow e^- \bar{\nu}_e N) \frac{\Gamma(N \rightarrow \mu^+ \mu^- \bar{\nu}_\mu)}{\Gamma_N}, \end{aligned} \quad (14)$$

$$\begin{aligned} & \Gamma(\tau^- \rightarrow \{\pi^-\}_1 \{\mu^+ \mu^- \nu\}_2) \\ & \approx \delta_N \cdot \Gamma(\tau^- \rightarrow \pi^- N) \frac{\Gamma(N \rightarrow \mu^+ \mu^- \bar{\nu}_\mu)}{\Gamma_N} \\ & + \Gamma(\tau^- \rightarrow \pi^- N) \frac{\Gamma(N \rightarrow \mu^+ \mu^- \nu_\mu)}{\Gamma_N}. \end{aligned} \quad (15)$$

As noted before, we do not make distinctions of a final neutrino or antineutrino of any flavor since they are not identifiable experimentally. The corresponding branching ratios with the latter vertex topologies and consistent with Eq. (1) are in the range:

$$\text{Br}(\tau^- \rightarrow \{e^- \nu\}_1 \{\mu^+ \mu^- \nu\}_2) < 1.6 \times 10^{-5}, \quad (16)$$

$$\text{Br}(\tau^- \rightarrow \{\pi^-\}_1 \{\mu^+ \mu^- \nu\}_2) < 1.3 \times 10^{-5}. \quad (17)$$

Unlike the former topologies, these ones are not bounded from below. This is as a consequence of the presence in (14) and (15) of a global factor  $|U_{\tau N}|$  unbounded from below. Consequently, experimental nonobservation of these processes cannot rule out sterile neutrinos in the range stated in Eq. (1). The same conclusion applies to the like-sign dilepton processes  $\tau^- \rightarrow \mu^- \mu^- \pi^+ \nu$  and  $\tau^- \rightarrow \mu^- \mu^- e^+ \nu \nu$ . In fact, their branching ratios are in the range:

$$\text{Br}(\tau^- \rightarrow \{\mu^- \nu\}_1 \{\mu^- e^+ \nu\}_2) < 1.3 \times 10^{-5}, \quad (18)$$

$$\text{Br}(\tau^- \rightarrow \{\mu^- \nu\}_1 \{\mu^- \pi^+\}_2) < 8.2 \times 10^{-5}, \quad (19)$$

also not bounded from below.

Another issue to take into account in the  $\tau$  decays of Eq. (5) concerns the probability  $P_N$  for the neutrino  $N$  to decay inside the detector. Roughly, for a detector of length

$L_D$ , the probability  $P_N$  takes the form  $P_N \approx 1 - e^{-L_D/L}$ , where  $L = \gamma c \tau_N$  is the decay length of the sterile neutrino. Assuming  $\gamma = 1$ , the decay length  $L$ , within which  $\sim 63\%$  of the sterile neutrinos decay, is

$$L = 0.6\text{--}30 \text{ cm}. \quad (20)$$

The most sensitive detectors to the  $\tau$  decays in Eq. (5) are SuperB [19], Belle [20], BABAR [21], CLEO-c [22] and BES-III [23]. In particular, BABAR and Belle have  $4.9 \times 10^8$  and  $7.2 \times 10^8$   $\tau^+ \tau^-$  pairs of events, respectively [24], which for clean signals correspond to a sensitivity for the  $\tau$  branching ratios of the order of a few times  $10^{-9}$ .

Then, considering that the decay length  $L$  in Eq. (20) is smaller than the detector sizes, and that the branching ratios in Eq. (16) and (17) are within the reach of BABAR and Belle, we conclude that displaced vertex searches of  $\tau$  decays in Eq. (5) should be able to test the sterile neutrino scenario corresponding to the parameters given in Eqs. (1), (2), and (4), proposed as a nonoscillation explanation of the MiniBooNe anomaly. We understand that these searches have not been done, in particular, by BABAR so far, but in principle they should be feasible [25].

A last comment is in order. In principle, the contribution of a sterile neutrino can also be searched for in radiative decays  $\tau^- \rightarrow \mu^- \nu \nu \gamma$ , taking into account that in the studied scenario its dominant decay is precisely  $N \rightarrow \nu \gamma$ . Consequently, the search for displaced vertices  $\tau^- \rightarrow \mu^- N$  and  $N \rightarrow \nu \gamma$  should give a larger signal. However, reconstruction of the secondary vertex  $N \rightarrow \nu \gamma$  represents a significant difficulty for the above-mentioned experiments [25].

In summary, we suggest that searches for the rare  $\tau$  decays  $\tau^- \rightarrow \mu^- \mu^+ \pi^- \nu$  and  $\tau^- \rightarrow \mu^- \mu^+ e^- \nu \nu$  exhibiting displaced vertices (i.e. a primary vertex where  $\mu^-$  is produced and a secondary vertex where the pair  $\mu^+ \pi^-$  or  $\mu^+ e^-$  is produced, respectively), should constitute tests for the existence of a massive sterile neutrino with parameters in the range shown in Eqs. (1), (2), and (4), required to explain the MiniBooNE anomaly without neutrino oscillations. These searches could be done with already existing experimental data.

We are grateful to Ignacio Aracena, Hayk Hakobyan, and Will Brooks for useful discussions. We also thank Sergey Gninenko and Alberto Lusiani for useful comments. J. C. H. thanks the IFIC for hospitality during his stay. This work was supported by FONDECYT (Chile) under projects 1100582, 1100287; Centro-Científico-Tecnológico de Valparaíso PBCT ACT-028, by Research Ring ACT119, CONICYT (Chile), and CONICYT/CSIC 2009-136. M. H. acknowledges support from the Spanish MICINN Grants FPA2008-00319/FPA, FPA2011-22975, MULTIDARK CSD2009-00064, and 2009CL0036, and by G. V. Grant Prometeo/2009/091 and the EU Network Grant UNILHC PITN-GA-2009-237920.

- [1] A. Aguilar *et al.*, *Phys. Rev. D* **64**, 112007 (2001), and references therein.
- [2] A. A. Aguilar-Arevalo, *Phys. Rev. Lett.* **102**, 101802 (2009).
- [3] A. A. Aguilar-Arevalo *et al.*, *Phys. Rev. Lett.* **102**, 101802 (2009), and references therein.
- [4] E. Zimmerman (MiniBooNE), PANIC, 2011; Z. Djurcic (MiniBooNE), NUFACT, 2011.
- [5] A. Donini, P. Hernandez, J. Lopez-Pavon, and M. Maltoni, *J. High Energy Phys.* **07** (2011) 105; C. Giunti, arXiv:1110.3914; C. Giunti and M. Laveder, *Phys. Rev. D* **84**, 073008 (2011); C. Giunti, arXiv:1106.4479; J. Kopp, M. Maltoni, and T. Schwetz, *Phys. Rev. Lett.* **107**, 091801 (2011); M. Maltoni, *et al.*, *Nucl. Phys.* **B643**, 321 (2002); M. Maltoni, T. Schwetz, and J. W. F. Valle, *Phys. Lett. B* **518**, 252 (2001); A. Ioannisian and J. W. F. Valle, *Phys. Rev. D* **63**, 073002 (2001); M. Hirsch and J. W. F. Valle, *Phys. Lett. B* **495**, 121 (2000).
- [6] S. N. Gninenko, *Phys. Rev. Lett.* **103**, 241802 (2009).
- [7] S. N. Gninenko, *Phys. Rev. D* **83**, 015015 (2011); S. N. Gninenko, *Phys. Rev. D* **83**, 093010 (2011).
- [8] B. J. P. Jones, arXiv:1110.1678; C. M. Ignarra, arXiv:1110.1604.
- [9] The model is in agreement with the latest MiniBooNE results; Sergei Gninenko (private communication).
- [10] See, for example, R. N. Mohapatra and P. B. Pal, *Massive Neutrinos in Physics and Astrophysics* (World Scientific, Singapore, 1991).
- [11] See, for example, M. A. Acero, C. Giunti, and M. Laveder, *Nucl. Phys. B, Proc. Suppl.* **188**, 211 (2009).
- [12] C. Giunti and M. Laveder, *Phys. Rev. D* **84**, 093006 (2011).
- [13] C. Dib, *et al.*, *Phys. Rev. D* **84**, 071301(R) (2011); M. Masip and P. Masjuan, *Phys. Rev. D* **83**, 091301 (2011) arXiv:1103.0689. D. McKeen and M. Pospelov, *Phys. Rev. D* **82**, 113018 (2010); E. Ma, G. Rajasekaran, and I. Stancu, *Phys. Rev. D* **61**, 071302 (2000); E. Ma and G. Rajasekaran, *Phys. Rev. D* **64**, 117303 (2001); S. Palomares-Ruiz, S. Pascoli, and Th. Schwetz, *J. High Energy Phys.* **09** (2005) 048.
- [14] V. A. Duk, *et al.* (ISTRA+ collaboration) arXiv:1110.1610.
- [15] S. N. Gninenko and D. S. Gorbunov, *Phys. Rev. D* **81**, 075013 (2010).
- [16] A. Atre, T. Han, S. Pascoli, and B. Zhang, *J. High Energy Phys.* **05** (2009) 030.
- [17] C. Dib, V. Gribov, S. Kovalenko, and I. Schmidt, *Phys. Lett. B* **493**, 82 (2000); J. C. Helo, S. Kovalenko, and I. Schmidt, *Nucl. Phys.* **B853**, 80 (2011).
- [18] J. C. Helo, S. Kovalenko, and I. Schmidt, *Phys. Rev. D* **84**, 053008 (2011).
- [19] M. E. Biagini *et al.* (SuperB Collaboration), arXiv:1009.6178.
- [20] A. Abashian *et al.*, *Nucl. Instrum. Methods Phys. Res., Sect. A* **479**, 117 (2002).
- [21] B. Aubert *et al.* (BABAR Collaboration), *Nucl. Instrum. Methods Phys. Res., Sect. A* **479**, 1 (2002).
- [22] D. Peterson *et al.*, *Nucl. Instrum. Methods Phys. Res., Sect. A* **478**, 142 (2002).
- [23] D. M. Asner *et al.*, *Int. J. Mod. Phys. A* **24**, 499 (2009) arXiv:0809.1869.
- [24] K. Hayasaka, arXiv:1010.3746; A. Pich, *Nucl. Phys. B, Proc. Suppl.* **186**, 187 (2009).
- [25] Alberto Lusiani (private communication).